SPE 128873

Case Study of the Impact of Cold and Hot Waterflooding Performance by Simulation and Experiment of High Pour Point Oil Reservoir, Liaohe Oilfield, North-East China

Zhou Wei, Tang Zhong-hua, China University of Geosciences, Wuhan, China, Orodu Oyinkepreye D., SPE, Covenant University, Ota, Nigeria

This paper was prepared for presentation at the SPE Oil and Gas India Conference and Exhibition held in Mumbai, India, 20–22 January 2010.

Abstract

Block Shen-95 has been under cold waterflooding for 17 years. Of particular interest is the low recovery of 11.27% for the North Block due to crude oil cloud point being very close to the reservoir temperature. Formation damage near the wellbore region is controlled at production wells by hot-oiling and low injection rates of non-isothermal waterflooding.

Optimizing production necessitated looking at core-scale experiment and reservoir-scale simulation waterflooding performance at different temperatures. The intent also, is basically to condition core-scale flooding observations to properly initialize the numerical model. Based on experiment carried out on core samples, sharp decline in oil displacement efficiency occurred, increase in residual oil saturation and increase in the intensity of formation damage below the cloud point. Reservoir simulation depicted decline in production with decreasing flooding temperature captured specifically by change in viscosity around the wellbore region. Change in flow dynamics due to change in relative permeability was not efficiently captured and formation damage impact on porosity and permeability.

Reservoir-scale performance for high pour point oil reservoir can better be understood by considering the effects of formation damage on storativity and transmissibility, and fluid rheology. The irreversible process of wax precipitation may cause permanent damage if further from the wellbore region.

Introduction

Block Shen-95 has been under cold waterflooding for 17years of the 23years in which the oil-block have being on production. Oil recovery for the North Block is 11.27% and South Block is 14.99%. Recovery is low as a result of average crude oil cloud point being close to the reservoir temperature. Furthermore, flooding pattern of inverted 9-spot and 5-spot for both blocks respectively have affected recovery. Pertinent issue is prevention of formation damage near wellbore region at production wells by hot oiling at injection wells by low injection rates to prevent paraffin crystallization, precipitation and deposition with adverse effect to optimal flooding.

Prior study[1] after commencement of full development and initiation of secondary recovery had suggested non-isothermal flooding will have adverse effect and suggested enhanced recovery schemes of hot waterflooding and polymer flooding. Studies of non-isothermal flooding had brought to fore the effect on fractional flow due to change in viscosity causing adverse mobility ratio and the establishment of a cold water bank with increase in skin effect[2,3,4] and reservoir damage. Sweep efficiency is considerably affected at the later flooding stage from 1-D displacement analytical and graphical methods taking into cognizance paraffin precipitation[5]. Other influence includes change in wettability from water-wet to oil-wet and variation in end-point saturation[6,7,8]. Experimentally, the influence of non-isothermal (cold) waterflooding has been acknowledged to cause increased water saturation and relative permeability for flooding below cloud point temperature[9]. For Shen-95, crude oil is characterized as having high point (42-60^{0}C); wax, 37%; resin and asphaltene, 12-20%; API^0 gravity, 25.8-36.25 and cloud point of 58.5-63^{0}C. This brings to fore the window of paraffin crystallization and precipitation with the resulting consequences of non-isothermal flooding as highlighted above.

This paper covers results and analysis of experimental core flooding at different temperatures at establishing isothermal flooding towards enhancing displacement and recovery as well as field-scale simulation at depicting experimental performance and monitoring performance by forecasting to optimize production in view of justifying hot waterflooding devoid of economic analysis.

Geological Setting

Block Shen-95 is located in Liaohe basin in the Jinganbao oil-bearing structure belt of Damintun depression in Xinmin city, Liaoning Province, North-East China. The block is an anticline faulted structure with oil-bearing strata dipping in the northwest direction with major axis 6.8km and minor axis 3.3km within an area of 16.9km^2. Based on the fault system the block is either subdivided into two sub-blocks North Fault Block and South Fault Block with respect to a major sealing fault in the NE direction or 4 sub-blocks by other major faults (see Fig. 1). The block has a complex system of faults with sealing, partial sealing and non sealing faults (faults are either normal or growth faults). S_3^4 segment, the oil-bearing segment is of the Shahejie Formation of the Paleogene period (Eocene). The oil-bearing segment interval is approximately within the range 1800-2230m subsurface depth with average porosity of 19% and low permeability of 3mD. The reservoir depositional environment belongs to the fluviodeltaic depositional system with relatively small sand body and complex depositional structure. There are 12 depositional sedimentary environments or sedimentary micro-facies.

Deposition is marked by regression with upward coarsening. From sequence stratigraphy of unpublished report the reservoir is subdivided into 3 Zones of 20 layers or 17 layers for the subsurface under region under investigation. The 17 layers subdivision is adopted based on data availability of "effective oil thickness" herein referred to as Net-Pay (NTG) and the 20 layers subdivision is integrated into it since depositional facies framework is in this nomenclature. The layers are heterogeneous with high variation in thickness and poor horizontal connectivity. Production is supported by high injection pressure having low injection efficiency, and the reservoir pressure is low being slightly higher than saturation pressure. The reservoir consists of no gas cap, but has edge water with no bottom water at the top part of the reservoir, and alternating sequence of oil-water interval. Formation water is composed essentially of fresh water.

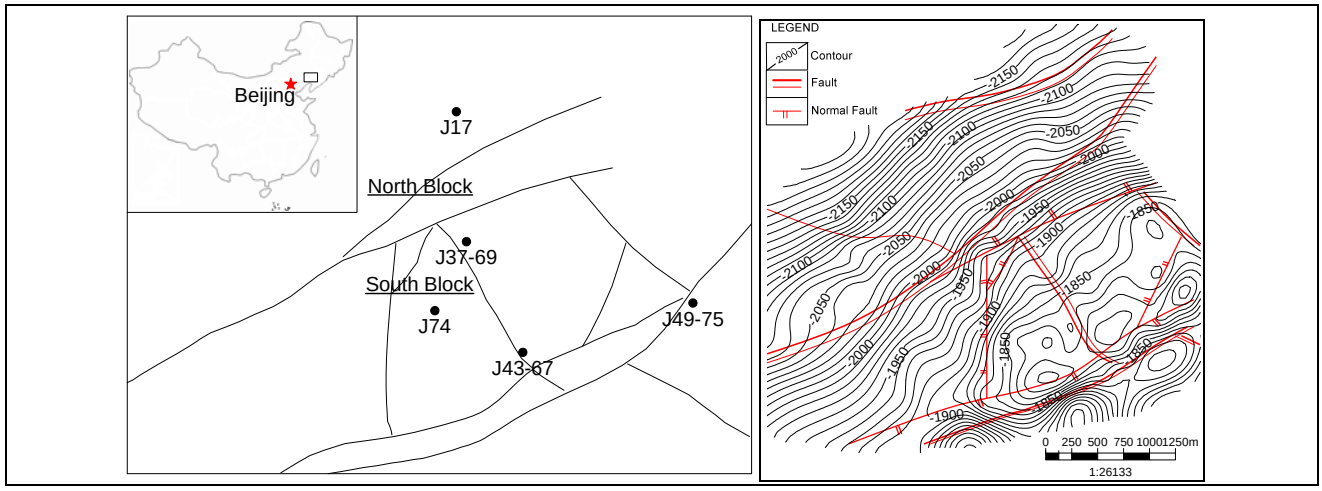

Fig. 1: Block Shen-95 (a) showing cored wells location and faults and (b) reservoir top surface.

Core-Scale Waterflooding

The difference between high pour point and general oil reservoir is the characteristics of high pour point oil due to its high was content having relatively high cloud point that is close to or higher than initial reservoir temperature. Hence, isothermal and/or hot waterflooding has to be considered for effective field development.

Fluid Characteristics

Viscosity-Temperature

High pour point oil viscosity-temperature curve is very sensitive to temperature based on observed dead-oil viscosity-temperature curves above and below the cloud point range. The change is relatively small above cloud point (Wax precipitation temperature - WPT) (Fig 2 viscosity-temperature curve). Temperature is very sensitive to wax. The crude oil is in the liquid state for temperature above pour point, solid-state below pour point although some wax is liquid-state due to wax crystallization and precipitation. So, 5 temperatures of 50^0C (below WPT), 63^0C (WPT highest range, and above this temperature flow is Newtonian, Fig 3, against pseudo-plastic with adverse mobility), 70^0C, 80^0C and 90^0C are chosen for core flooding.

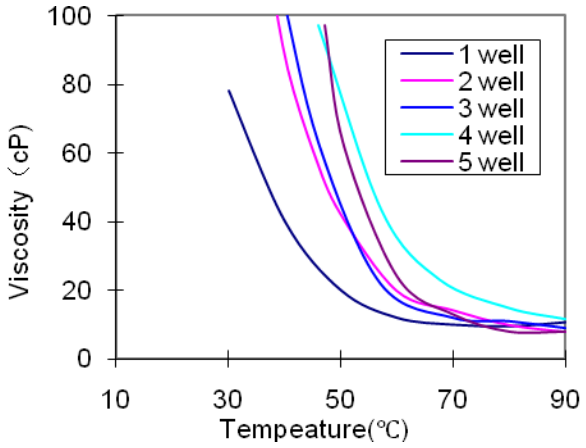

Fig. 2: General Viscosity-Temperature curves of Jinganbao oil bearing structure belt of Damintun depression

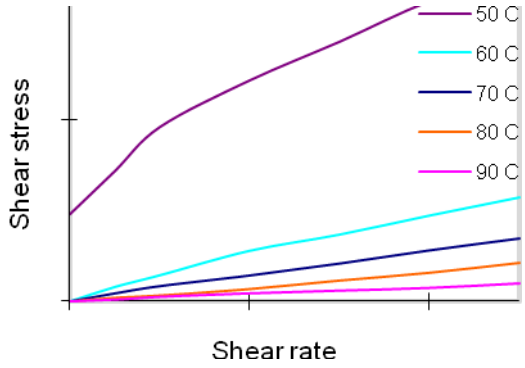

Fig. 3: Oil rheology, Well J33-75

Wax Precipitation Temperature

At this temperature wax crystals first starts to form and crude oil is saturated with wax resulting in high wax precipitation below this temperature as it is supersaturated. This point onwards, as temperature declines the fluid rheology change from Newtonian to non-Newtonian, so, WPT is important. WPT is related to;

- Number of carbon atoms in wax molecules (C17 ~ C70 alkyl group), and the higher the carbon atoms the higher the WPT and vice-verse however this phenomenon is irreversible.
- Pressure; at reservoir condition, dissolved gas content varies with pressure causing change in WPT. Below saturation pressure wax precipitate with pressure increase. However, at saturation pressure wax precipitation is lowest and so it is beneficial for reservoir development.

Experimental Design

The experiment consists of studying the characteristics of water displacement at different temperatures. The experiment is conducted according to;

1. Core flooding of four parallel samples at different temperatures.
2. Same core samples as above totalling 7 core samples are flooded
    a. 2 core samples are flooded at 55^0C, 60^0C, 67^0C and 70^0C
    b. 1 core sample flooded at 50^0C, 60^0C and 70^0C
    c. 1 core sample flooded at 60^0C and 70^0C
    d. The last 3 core samples are flooded at same temperature
    e. 2 core samples are flooded at each time from high to low temperatures, and 2 core samples are from low to high temperatures.
3. Simulated long cores flooded at different temperatures

Results and Discussion

Water Displacement at Different Temperatures

The first type of experiment of 4 parallel core samples were displaced by water at 550C, 600C, 660C and 760C and result presented for water free production (Table 1) with increasing displaced oil in accordance with increasing flooding temperature. Second type of experiment with same core samples and results presented, Table 2, for free water production, 98% water-cut and final (ultimate) recovery showing similar trend like prior experiment.

Table 1: Oil displacement efficiency at different temperatures

Water Injection Oil Dis. % Time / Temperature ^{0}C	Water Free production	0.5	1.0	2.0	10	Final
70^{0}C	37.42	42	47	50.2	57.0	63.23
65^{0}C	25.76	36	40	44.0	48.5	53.86
60^{0}C	23.42	32.0	37.5	41.0	45.0	46.84
55^{0}C	14.05	22.5	25.4	28.0	35.5	42.15

For the simulated water injection case with designed artificial 30cm long and 2.5cm diameter core sample, held at formation temperature, the result of displaced oil efficiency increases with increase in injection temperature (Table 3).

Table 2: Oil displacement efficiency

Temperature / Displacement / Core Sample	Oil Displacement Efficiency				Water-cut 98% Oil Displacement Efficiency				Final Displacement Efficiency			
	55^{0}C	60^{0}C	65^{0}C	70^{0}C	55^{0}C	60^{0}C	65^{0}C	70^{0}C	55^{0}C	60^{0}C	65^{0}C	70^{0}C
J43-67(1881.0m)	24.37	33.90	34.48	34.0	30.85	36.38	48.22	49.80	31.09	36.44	48.28	54.00
J74 (2002.5m	27.50	36.84	41.08	45.07	41.87	49.25	52.35	55.15	42.50	55.26	55.41	56.34
J37-69(2004.9m)		12.50	14.71	17.14		24.49	30.50	35.52		31.25	41.18	42.86
J74(1896.0m)			12.00	10.42			36.79	41.22			38.00	45.83

Table 3: Oil Displacement efficiency of long cores

Core	Free Water Production				Final Displacement			
	55^{0}C	60^{0}C	65^{0}C	70^{0}C	55^{0}C	60^{0}C	65^{0}C	70^{0}C
J74(1921.5m)	4.81	6.31	9.89	12.92	44.93	45.12	49.50	55.84
J43-67(1925.5m)	8.80	14.46	19.33	38.10	44.82	45.33	50.64	

Oil displacement efficiency below WPT is lower in all cases with much less increase from free water production to 98% water-cut for case-2 experiment (Fig 4). The trend in Fig. 4 is similar for all cores with sharp decline in displacement efficiency below WPT. Oil permeability computed at 70^{0}C, 60^{0}C and 55^{0}C are 644mD, 131mD and 109mD respectively. Permeability is lower for flooding temperatures below WPT of (58.5-63^{0}C) at average value of 60^{0}C showing wax precipitation below WPT. Viscosity, not only increasing, but paraffin deposition in pore space resulting in decreased permeability and reduced oil displacement efficiency.

Relative Permeability Curves at Different Temperatures

Fig 5 shows the interpretation of the shift of the oil-water relative permeability curves with respect to increase in temperature of flooding. The span of the oil-water relative permeability curve increases, residual oil saturation decreases and irreducible water saturation change, these affects the relative permeability curve. In few words, temperature has a great impact on the high pour point oil displacement efficiency with water-cut increasing slowly.

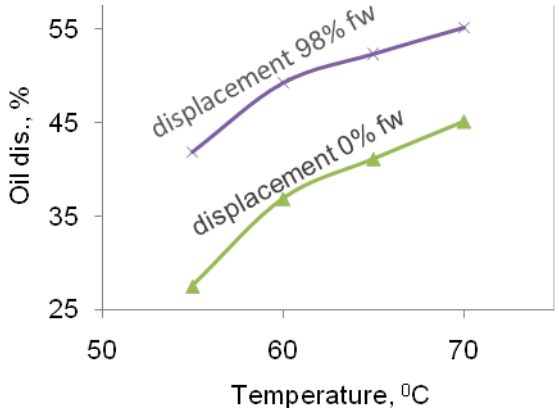

Fig. 4: Oil displacement efficiency, J74 (2002.5m)

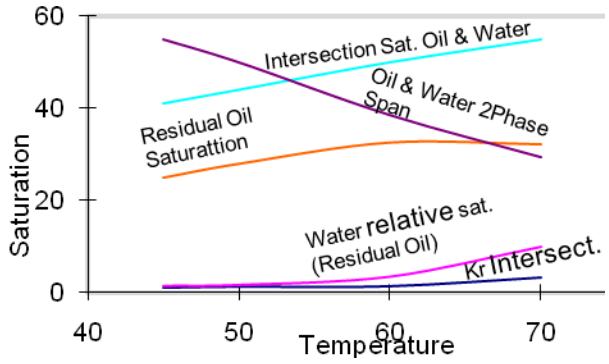

Fig. 5:Relative permeability curve parameter Well J43-67 variation with temperature

Evaluation of Formation Damage

With reduction of core flooding temperature to WPT and below, wax precipitated from crude oil. Wax exist in the pore network causing reduced pore throat aperture, reduced porosity and permeability, and reduced displacement efficiency.

- Effect on aperture: average pore throat diameter reduced from an average of 11µm at initial temperature of 70^{0}C to 7.94µm at 63^{0}C representing 27.6% decline
- Effect on porosity: average porosity of 32.3% at initial temperature of 70^{0}C to 16.3% at 63^{0}C with a 15.3% decrease in porosity.
- Effect on permeability: as earlier mentioned above, substantial reduction occurred in porosity and aperture therefore resulting in decline of formation permeability. Average permeability of 1300mD at 70^{0}C reduced to 365mD showing a decrease of 72%.
- Impact on oil displacement efficiency: efficiency reduced from 68.7% at initial temperature of 70^{0}C to 54.0% at 63^{0}C and further down to 34.3% at 58.5^{0}C.

The injection of cold water for the exploitation of high pour point below WPT results in wax crystallization, precipitation, entrainment and deposition causing blockage of small pore throat and a large change in formation porosity and average aperture. On the other hand, temperature reduction below pour point leads to a semi-solid state and rapid deterioration of flow. Hence, it is obvious that cold water injection leading to temperature at pay zone being below WPT will damage the formation at near wellbore region.

Reservoir Simulation Isothermal and Non-isothermal Waterflooding

This simulation study was meant to capture the influence of isothermal and non-isothermal waterflooding under prediction mode by observing performance based on history match simulation model. The strong influence of viscosity variation with temperature below and above WPT affects mobility and flooding performance. Porosity and permeability reduction below WPT is not considered so as the direct effect on relative permeability and non-Newtonian flow below WPT. Change in relative permeability with change in residual oil saturation is accounted for. As such, temperature change updated by the solution of the energy balance after that of the flow equations is the basis for updating viscosity at each time step. So, rock and fluid properties controls heat transfer. Injection temperature at pay zone is obtained based on geothermal gradient and injection rate.

Apart from, viscosity variation with temperature, the other effect of temperature decline below WPT with time could not be efficiently accounted for with the Black-Oil simulator used.

Reservoir Model for Simulation

The reservoir model used for simulation was based on the defined faults, reservoir top and 17 layers, depositional facies (depositional environment), effective sand thickness from existing geological model, and computed permeability, porosity and water saturation from correlations at well locations. The 12 depositional facies were grouped into 6 depositional facies based on reasonable porosity trends (variation). These were distributed in the 3D grid structure using the commercial software's interactive facies modelling workflow tool. The same software was used for reservoir modelling. The upscaled grid structure for the North Block has 61,710 cells (110×33×17) of Δx, 50m; Δy, 50m; and Δz in accordance with the 17 layers; and for the South Block, 113,152 cells (104×64×17) of Δx, 50m; Δy, 50m; and Δz in accordance with the 17 layers. The x and y cell dimension of the grid was chosen to enable simulation with less computing storage capacity and speed, consideration for the high number of wells with similar/common well-log responses and also the average minimum of two cells between cells penetrated by wells.

"Effective sand thickness/net sand" was digitized and assigned to cells and NTG computed from the division of "effective sand thickness" by cell-height. Well assigned porosity, permeability and water saturation were assigned to cells by arithmetic averaging upscaling for porosity and water saturation and geometric averaging for permeability. The various properties of cells penetrated by wells were distributed by sequential Gaussian Simulation algorithm, but for porosity, it was conditioned to the 6 grouped depositional facies, permeability model enhanced by porosity as a secondary variable.

Model Initialization and Description

The reservoir model was initialized by incorporating recurrent data of observed oil, gas and water production rates and water injection rates (50 wells including 9 horizontal, with well completion and intervention data for the North Block) as only the North Block is considered for simulation study. There were no perforation data for the horizontal wells, so in other to get a representative numerical model and/or result close to the real subsurface situation the horizontal wells were all arbitrarily perforated on the horizontal leg. Other data are pressure surveys, fluid and reservoir properties (Table 4), equilibrium tables, physical property constants, k_v/k_h (average of 0.001 for the North Block) and the initial water saturation model. Water PVT properties and rock compressibility were derived from correlation. While the pressure equilibrium table consist of Shen-95 reservoir pressure at 1800m and that of the reservoir below, 28.73MPa at 2300m. This is a normal pressure gradient. An aquifer is not considered as the reservoir is of low natural pressure support. Other initialized fluid and rock properties are those influencing heat transfer needed for energy conservation.

Study on the existence of barrier to flow was not successful as attempts to distribute shale identified at wells did not yield any continuous streak across the horizontal plane. However, shale distribution was higher at the reservoir top compared to either the mid or bottom of the reservoir and prior study identified coal embedded in mudstone at the reservoir top.

A Black-oil simulator was used based on a dead oil model with the basic 3D-grid consisting of porosity, permeability and NTG imported from the reservoir model. The grid dimensions are 110×33×17 for the North Block.

Table 4: Summary of reservoir and fluid properties

Reservoir depth	1800-2230m
Reservoir temperature	70^0C
Average porosity	19%
Average permeability	3mD
Net pay; North Block	12.2m
Initial reservoir pressure @ 1800m	17.98MPa
Initial bubble point pressure	11.8MPa
Initial oil saturation	66.3%
Initial GOR	$70m^3/t$
Initial oil boiling point	$127\text{-}132^0$C
Oil formation volume factor	1.134
Oil density	$0.8435\text{-}0.8991g/cm^3$
Pour point	$42\text{-}64^0$C
Viscosity @ 100^0C	3.83-9.67mPa.s
Average Cloud point	60^0C
Paraffin content	37.5%
Colloid + Asphaltene content	12-20%

Isothermal and Non-isothermal Waterflooding

Figure 6 show reasonable and acceptable history match for the North Block by adjustment through local refinement by scaling of relative permeability, residual oil saturation, sensitivity of vertical to horizontal permeability ratio, Net-to-gross, and pore volume. For individual well match, 21% were very good and 26 % were good. The initial high water-cut that was not matched is largely due to a well which was eventually converted to an injection well that was perforated close to a water zone.

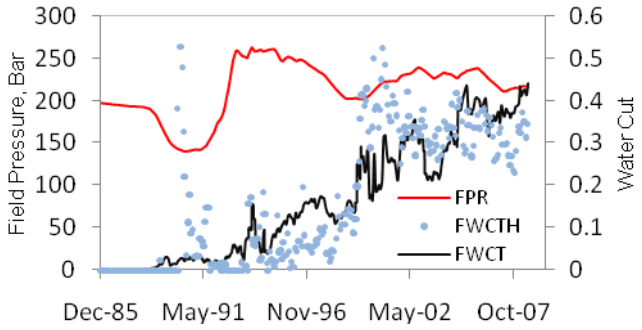

Fig. 6: Block Shen-95 North Block water-cut match

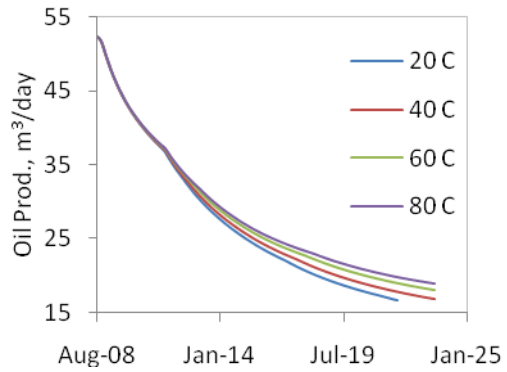

Fig. 7: Injection temperature effect on predicted oil production

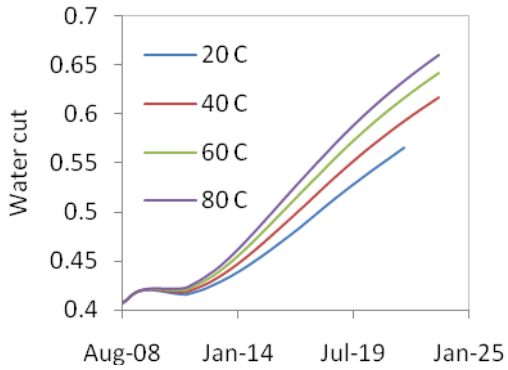

Fig. 8: Injection temperature effect on predicted water cut

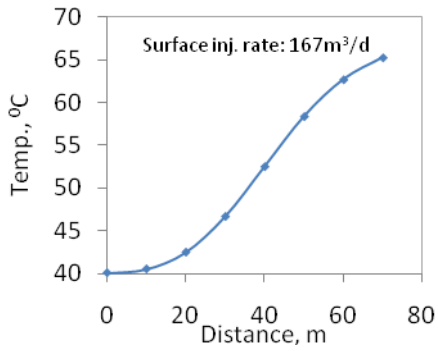

Fig. 9: Injection temperature rise with distance

Examination of isothermal and non-isothermal waterflooding is based on inverted 5-spot flood pattern although localized but different from the original inverted 9-spot pattern of which some injection wells had seized to exist at end of production history. Hence, some production wells were converted to injection wells for this purpose. Injection rates were maintained at 72m^3/day and pay zone injection temperatures carried out from 20^{0}C to 90^{0}C. Figures 7 and 8 present performance for produced oil and water-cut with favourable oil production with increase in injection temperature and likewise increase in water cut. This is a clear case of change in mobility ratio due to viscosity change, albeit, largely localized to the injection well cell block of 50m × 50m (simulation) grid. This is shown from the increase in temperature around the wellbore region for a simulated case of the fine grid (10m × 10m) for injection rate of 167m^3/day and 40^{0}C (Fig. 9). The plot of Fig. 9 depicts a short injection period of about 6 months, however for a long period the rise will be slow as represented by the further difference in predicted rates and water-cut of Fig 7 and 8 due to mobility change necessitated by increase in viscosity away from the wellbore and wellbore region. A smaller grid size would have had a different result with faster increase in temperature of the cell blocks penetrated by the injection well and near wellbore region with drastic change in viscosity, mobility and production.

Discussion

The core-flooding experiment shows the consequences of non-Isothermal flooding, especially below the wax precipitation temperature (WPT). Paraffin precipitation is irreversible, hence field scale prevention had being confined to the economical method of injection rate reduction at ambient temperature flooding with the aid of geothermal heating for temperature rise from the wax precipitation temperature. Temperature influence on the crude oil physical properties and the impact on subsurface fluid dynamics and formation had being properly quantified.

The drastic implications of flooding below WPT as observed and interpreted applies to near wellbore region and cells penetrated by injection wells which may further migrate beyond this range/region depending on flooding duration, injection rate and temperature. Based on the black-oil simulator used, the influence of injection below WPT observed in core flooding could only be applied due largely to the variation of viscosity and minimally to residual oil saturation to an extent. Neither the influence on formation damage of porosity reduction and pore throat reduction nor permeability reduction, as it extends from the wellbore to the formation could be adequately depicted. Known studies on the influence of non-isothermal injection are focused on additional skin effect[2,3], displacement efficiency[5] and rheological property of viscosity and Newtonian flow (also non-Newtonian flow) and its influence on productivity built into a numerical simulation model for the North Block also called Jing-17 reservoir[10]. And, using a commercial simulator as in this study, Mezzomo and Rabinovitz[11] considered the influence of paraffin with temperature by the sensitivity of residual oil saturation. So a holistic approach at studying the influence of non-isothermal water flooding still remains with quantifying the true effect of formation damage below WPT for a simulated field case and the effect of dissolved gas apart from the effect on a dead-oil study.

Conclusion

The effect of waterflooding below the wax precipitation temperature and hot waterflooding above this temperature is established at the core scale from experimental study on displacement efficiency, formation damage and relative permeability. Improved recovery had been replicated at field scale study for the North Block of Block Shen-95 for flooding at different temperatures. However, only viscosity effect had been adequately modelled without capturing formation damage as it affects permeability, porosity and relative permeability curves change with temperature. Improvement lies also by considering non-Newtonian flow below the cloud point, smaller grid size to adequately capture viscosity change with temperature especially near wellbore region to properly quantify performance for field scale study of high pour oil reservoirs.

References

1. Dou, H., Sun, P. (1995) “Technology used in the production of high pour point crude Oil in Shenyang Oilfield”, SPE 29953 presented at the SPE International Oil and Gas Conference and Exhibition in China held in Beijing, China, 14-17 November, 1995.
2. Platenkamp, R. J. (1985) “Temperature distribution around water injectors: Effects on injection performance”, SPE 13746, SPE Middle East Oil Technical Conference and Exhibition, Bahrain, 11-14 March, 1985.
3. Cassinat, J. C., Payette, M. C., Taylor, D. B. and Cimolai, M. P. (2002) “Optimizing waterflood performance by utilizing hot water injection in a high paraffin content reservoir”, SPE 75141, SPE/DOE Improved Oil Recovery Symposium, Tulsa, Oklahoma, 13-17 April, 2002.
4. Ramey, H. J. JR. (1962) “Wellbore heat transmission”, Journal of Petroleum Engineering, pp. 427-440.
5. Bedrikovetsky, P. (1997) “Improved waterflooding in reservoirs of highly paraffinic oils”, SPE 39083 presented at the SPE 5th Latin American and Caribbean Petroleum Engineering Conference and Exhibition held in Rio de Janeiro, Brazil, 30 August – 3 September, 1997.
6. Leontaritis, K J., Amaefule, J. O. and Charles, R. E. (1992) “A systematic aapproach for the prevention and treatment of formation damage caused by asphaltene deposition”, SPE 23810, SPE International Symposium on Formation Damage Control, Lafayette, LA, 26-27 February, 1992.
7. McDougall, S. R. and Sorbie, K. S. (1995) “The impact of wettability on waterflooding: Pore scale”, SPE Reservoir Engineering, August 1995, pp 20-213.
8. Civan, F. (2000) **Reservoir formation damage**, Gulf Publishing Company, Houston, Texas, pp. 67, 72.
9. Maloney, D. and Osthus, A. (2005) “Effects of paraffin wax precipitation during cold water injection in a fractured carbonate reservoir”, Petrophysics, Vol. 46 (5), pp. 354-360.
10. Qu, A., Tang, Z., Liao, D. And Lu, Z. 2006, Rhelogical properties of crude oil in Jing-17 Reservoir and its effects on productivity, Geological Science and Technology Information, Vol. 25(3), pp. 73-77 (In Chinese).
11. Mezzomo, R. F. and Rabinovitz, A., 2001. “Reservoir paraffin precipitation: The oil recovery challenge in Dom Joao Field?”, The Journal of Canadian Petroleum Technology, Vol. 40(6), pp. 47-53